

Drying Drops of Paint Suspension: From “Fried Eggs” to Quasi-Homogeneous Patterns

Stella M. M. Ramos,* Damien Soubeyrand, Rémy Fulcrand, and Catherine Barentin



Cite This: *Langmuir* 2023, 39, 13579–13587



Read Online

ACCESS |



Metrics & More

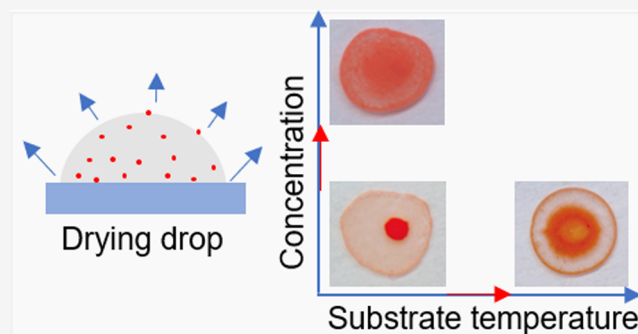


Article Recommendations



Supporting Information

ABSTRACT: Drying of multicomponent sessile drops is a complex phenomenon involving intricate mechanisms. Here, we study the evaporation of drops made of paint suspension and investigate the influence of the substrate temperature and suspension concentration on the resulting deposit patterns. At low concentrations and temperatures, the pigments appear highly concentrated in a narrow area at the center of the drop, a morphology we call “fried eggs”. Increasing the temperature or concentration leads to more homogeneous patterns. From a top-view camera used for monitoring the whole evaporative process, we identify three mechanisms responsible for the final pattern: *inward/outward flows* that convect the pigments, *gelation of the paint suspension* where pigments accumulate, and *final drying* of the drop that freezes the location of the pigments onto the substrate. The relative kinetics of these three mechanisms upon concentration and temperature govern the deposit growth and the morphology of the final pattern. These observations are quantitatively supported by rheological measurements highlighting a strong increase of the viscosity with concentration, consistent with the gelation mechanism. Finally, we show that the kinetics of drop drying is controlled by the substrate temperature.



INTRODUCTION

Evaporation of colloidal drops on solid surfaces and the resulting patterns have been studied for more than two decades with increasing interest in both fundamental research^{1–4} and practical applications.^{5–7} Many investigated systems are faced with the omnipresent effect of particle accumulation at the drop edge where it forms a ring-shaped deposit (the so-called “coffee-ring effect”), which can compromise the potential applications. The mechanism leading to this nonuniform deposition was established by Deegan et al.¹ who attribute the ring formation to a capillary flow that convects suspended particles to the drop’s edge. This flow can be, however, strongly impacted by numerous parameters (e.g., size and shape of the suspended particles,^{8,9} concentration,^{10,11} temperature and wettability of the substrate,^{12,13} etc.), which, usually, modify the final deposition of the suspended particles. Indeed, numerous factors create surface tension gradients in the evaporating drop, which induce Marangoni flow from the edge to the apex of the drop. In general, this flow partially or completely inhibits the outward flows and thereby ensures a recirculation of particles. Two contributions have to be distinguished: (i) solutal Marangoni flow induced by concentration gradients along the gas–liquid interface^{14,15} and (ii) thermal Marangoni flow induced by a temperature gradient along the gas–liquid interface.^{4,15} On this matter, different works^{12–16} pointed to significant alterations in the final deposition of colloidal drops evaporating on heated

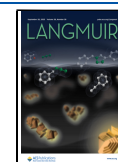
substrates due to an enhancement in the thermal Marangoni flow on hot surfaces. Examples of numerous studies can also be found in previous reviews^{16,17} where generating and controlling evaporative flows inside the drops appear as a key parameter to pattern colloids on surfaces in a controlled way.

A great part of such investigations deals, however, with model systems where the physical, chemical, and geometrical properties of the suspension are generally well controlled. In fact, the situation is largely more complex in the case of the evaporation of multicomponent drops (e.g., blood,^{18,19} biological fluids,²⁰ paint suspensions,²¹ etc.) where the physicochemical properties of the colloidal suspension are, sometimes, not completely established or even partially unknown. The nonuniform distribution of different components leads to a surface tension gradient, which usually modifies the drying dynamics. Moreover, the evaporation of complex fluids may induce modifications of the rheological properties of the suspension, such as a sol–gel transition,^{22,23} which affect the evaporative flows and thus the shape of the final pattern.

Received: June 13, 2023

Revised: August 23, 2023

Published: September 14, 2023



Despite numerous studies reported in recent reviews,^{17,24,25} the mechanisms behind the deposition morphology of multicomponent drops remain poorly understood. Numerous difficulties resulting from multiple physical phenomena are usually present in real systems.

In the field of paint suspension, the obtention of a homogeneous deposition (free of undesirable patterns, small cracks, etc.) can be faced with many difficulties. A great number of parameters involved (such as the multicomponents of drop suspension and their physicochemical and mechanical properties) are, in general, poorly known. Better control and understanding of the mechanisms governing the drying process of paint suspensions and their rheological properties present an undeniable interest for fundamental investigations. Recent studies deal with shrinkage, and the mechanical properties of drying oil paint²⁶ or mechanical properties of artists paint-dried²⁷ illustrate well the potential interest of the proposed investigations to practical applications.

In the present article, we experimentally study the drying of a drop made of a paint suspension and the morphology of the resulting patterns. We separately investigate the influence of two parameters: the suspension concentration and the substrate temperature ranging between 30 and 80 °C. In order to identify the main mechanisms responsible for the final pattern in such complex systems, we combine top-view and side-view videos of the drying drops, rheological characterizations of the paint suspension, and SEM analysis of the final deposits.

More precisely, we describe initially the samples and the experimental setup used to study the evaporation of the drops. In a second time, we present the results, obtained with the sessile drop method, highlighting the influence of both concentration and temperature on the drying process and on the morphology of the final deposits. These results are then analyzed, together with surface tension and rheological measurements of the paint suspension. In particular, the outward capillary and inward Marangoni flows are identified as well as a sol–gel transition of the suspension at the drop contact line, which grows with time toward the center of the drop. In the last part of this section, we discuss the influence of both concentration and temperature on the main processes at play and their relative kinetics. Finally, we conclude and show that the morphology of the final pattern can be controlled in a real complex system by key parameters, such as the concentration or the temperature.

EXPERIMENTAL METHODS

Suspension Preparation. Commercial water-based paint named Architecte “Mat absolu” from the Dulux Valentine company was used. According to its datasheet, it is a high-quality paint rich in resin (acrylic emulsion) and pigments. By diluting this paint with ultrapure water, we prepared five different suspensions with the following volume concentrations: $\phi = 1.7, 2.5, 3.1, 8.3,$ and 16.7% . Glass slices of 0.13 mm thickness from the Marienfeld Superior company, possessing small roughness, were used as substrates.

Droplet Deposition and Imaging. The sessile drop method was adopted to investigate the evaporation process of drops on the glass surfaces. In such experiments, the samples were introduced in a glass chamber with controlled temperature and humidity rates. A small drop (volume of 3 μL), initially at room temperature, was put onto substrates heated at three different temperatures (30, 50, and 80 °C). Prior to deposition, all suspensions were sonicated to avoid sedimentation and pigment aggregation. The relative humidity was set to $45 \pm 5\%$ at the beginning of the experiments. Both side- and

top-view images of the evaporating drops were recorded with a CCD camera operating with a scan rate of 15 fps. The recorded frames allow extracting the geometrical parameters of each drop (contact angle θ and contact radius R_c) and following the drop evolution over time. At least 10 different experiments were performed on each sample at different temperatures to ensure repeatability.

Characterization and Rheology Measurements. The surface morphology of drops after complete drying was examined using both an FEI (Nova Nano SEM450) scanning electron microscope (SEM) operated at 30 kV and a mechanical profilometer (Bruken DEKTAK XT) from the Institut National des Sciences Appliquées (INSA) at Lyon (France).

The surface activity of the paint suspensions was also characterized by measuring the surface tension. Based on the pendant drop method, these measurements were performed with a standard drop tensiometer Tracker from Teclis-Scientific.

The rheological properties of the paint suspensions were measured in a cone–plate geometry using an industrial rotating rheometer (Anton Paar, Physica MCR 301) equipped with a Peltier device to ensure precise control of the temperature.

RESULTS AND DISCUSSION

Evaporating Drops. A drop of paint suspension deposited on a glass (hydrophilic) surface spreads quasi-instantaneously until reaching an initial wetting area delimited by a well-defined contact radius, R_c , and a contact angle θ .

The time evolution of these two parameters on a substrate maintained at 30 °C is shown in Figure 1 for two different

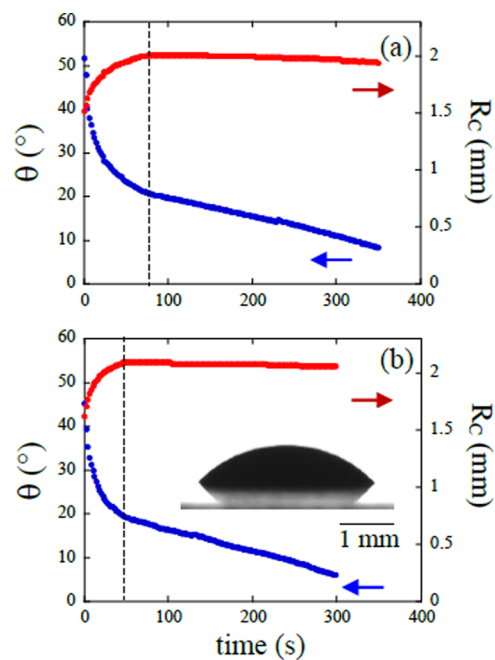


Figure 1. Time evolution of the contact angle θ and the contact radius R_c during the drop evaporation on glass surfaces at 30 °C. Volume concentration ϕ : (a) 2.5% and (b) 16.7%. Inset: instantaneous image (side view) of a typical drop at the end of the spreading stage.

concentrations. Qualitatively, it can be seen that the evaporation process is controlled by the contact angle dynamics. From Figure 1, two stages can be identified: a moving contact line regime (MCR) and a constant contact line regime (CCR). The first of these corresponds to the drop spreading, which ends when the contact radius reaches a maximal value and the contact angle reaches a critical value,

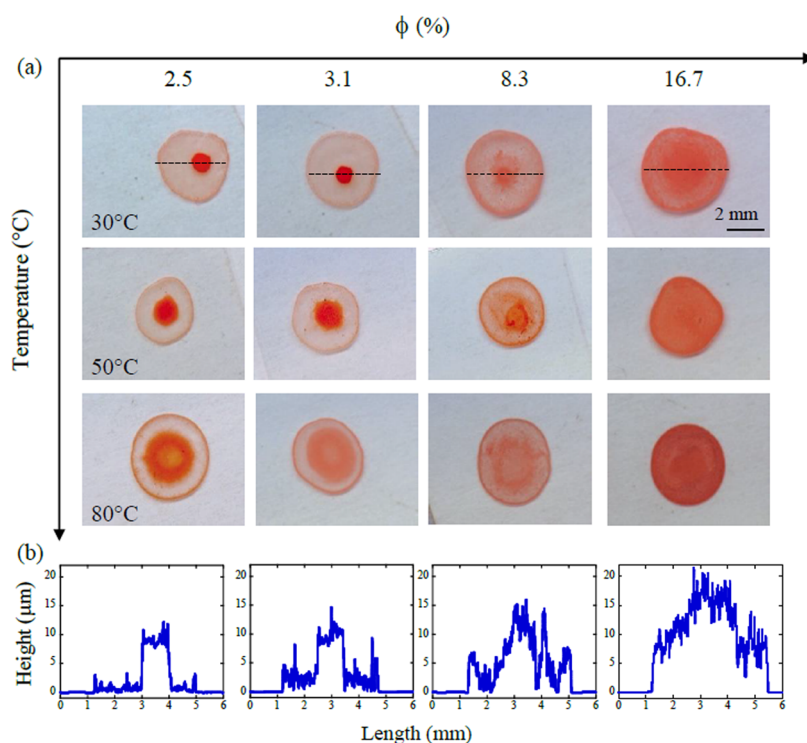


Figure 2. Morphology of the deposit after complete evaporation of drops made of paint suspension: (a) top-view images of the deposits obtained at different volume concentrations ($\phi = 2.5, 3.1, 8.3, 16.7\%$) and temperatures (30, 50, and 80 °C). (b) The height profile of the deposit was obtained at 30 °C, measured by a profilometry along the dashed lines shown in panel (a).

which in our experiments corresponds to an angle of $\theta = 21 \pm 2^\circ$. This is followed by a second regime (CCR) characterized by a quasi-constant contact radius and a strong contact angle decrease, resulting from the evaporation process. In this case, the drop evaporates with a constant contact area. Such behavior is due to the interaction between the components present in the paint formulation and the substrate. The pigments here act as anchorage points on the surface of the glass, inhibiting the contact line progress. In addition, as seen in Figure 1, increasing the suspension concentration leads to a decrease in the spreading time, accelerating the contact line pinning, whereas the drop dynamics and the contact angle value remain unchanged.

Pattern Formation. Figure 2 shows patterns obtained after the complete evaporation of the sessile drops. The shape of the final deposit depends on both suspension concentration and substrate temperature. To investigate the effect of the concentration on the final deposit shape, the top views of patterns on substrates at 30 °C are displayed in Figure 2a together with the height profile measured by a mechanical profilometer (Figure 2b). The data resulting from the profile analysis are reported in Table 1. From this analysis, it appears that for the lower concentrations ($\phi \leq 3.1\%$), a large proportion of pigments accumulate in a narrow area at the center of the drop, forming a well-defined stain. According to profile measurements, only an extremely thin ring-like residue of the particles is left at the drop edge. Both spot dimension and ring width increase with concentration. For $\phi = 8.3\%$, the final deposit consists of a larger central spot where the distribution of the pigments is less uniform and a relatively wide peripheral ring. For the highest concentration (16.7%), such a configuration evolves toward a quasi-homogeneous pattern characterized by a single enlarged stain whose height

Table 1. Main Geometrical Parameters Extracted from the Analysis of the Drop Profile Shown in Figure 2b^a

ϕ (μm)	2.5%	3.1%	8.3%	16.7%
W_R	65 ± 5	100 ± 20	415 ± 15	
H_R	2.7 ± 0.3	5.0 ± 0.8	6.5 ± 0.5	
D_{CS}	980 ± 50	1030 ± 20	2300 ± 40	4230 ± 20
H_{CS}	9.5 ± 1.5	10.5 ± 1.5	13.5 ± 2.0	18.5 ± 2.0

^aWidth W_R and height H_R of the ring, diameter D_{CS} and height H_{CS} of the central stain. The experiments were performed on substrates at 30 °C.

locally varies between 8 μm (at the edge) and 19 μm (in the central zone). It is worth here to mention that patterns showing only a single coffee ring, like previously reported by Deegan,³ were never observed in our experiments at any studied concentrations or temperatures. According to recent works,^{8,12} the particular shape and size of the suspended particles can completely avoid the coffee-ring effect.

In order to depict more precisely the structure of the different features constituting the final deposits, we performed SEM observations at high magnification. Typical top-view SEM images are shown in Figure 3. As can be seen, going from the center to the edge of the drop, four regions can be identified: a central region rich in pigments engulfed with acrylic paint (picture 1 in Figure 3). This region is successively surrounded by two other zones where the concentration of pigments radially decreases (pictures 2 and 3). Finally, a relatively wide ring resulting from the adsorption of the pigments on the solid surface is observed at the edge of the drop (picture 4).

To determine the dimensions of such elements, about 30 objects were measured, and their size was found in a wide interval varying from 0.5 to 7 μm . Their shape is in a great part

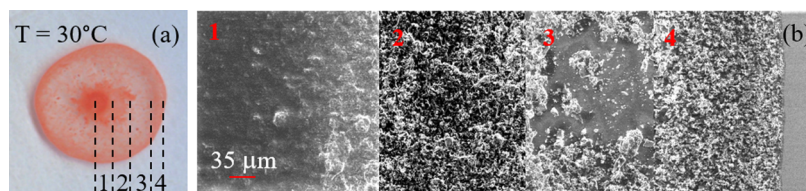


Figure 3. Top-view (a) and SEM images (b) of pigment distribution in the final dried drop at $\phi = 8.3\%$. Four different regions are identified.

irregular and anisotropic. They are found isolated or forming small packets of a few tens of micrometers in size. Such geometric characteristics could thus contribute to the pattern's morphology observed at low concentrations where the ring formation appears strongly attenuated.

Another striking feature, presented in Figure 2, deals with the effect of the substrate temperature on the resulting patterns. As can be seen, at $T = 50\text{ }^{\circ}\text{C}$, the final shape of pigment deposition appears to be affected little by the heating of substrates compared to the case at $T = 30\text{ }^{\circ}\text{C}$; only a slight increase in the size of the central stain is observed. The situation is different for drops with low paint concentrations at $T = 80\text{ }^{\circ}\text{C}$. In this case, pigments appear deposited in a combination of a large central area and an enlarged ring at the periphery of the drop that differs a lot from results obtained on the nonheated surfaces.

For the highest concentrations ($\phi = 16.7\%$), the weaker spatial mobility of pigments associated with accelerated evaporation renders their distribution more homogeneous. The influence of the substrate temperature on the diameter of the central stain D_{CS} and the diameter of the final dried drop D_{DD} formed by pigment deposition is reported in Figure 4a. It is shown that the central stain increases with the temperature, whereas the external diameter decreases at a much slower rate. From the plot of the diameter of central stains normalized by the size of the dried drop versus the temperature, displayed in Figure 4b, linear behavior is observed, evidencing the continuous growth of this central stain with temperature. Such an evolution can be understood considering that the external diameter is fixed by the pinning of the drop edge that takes place at the very beginning of the evaporation process.

Finally, our experimental results gathered in Figure 2a reveal that increasing the substrate temperature or suspension concentration leads to a more homogeneous distribution of pigments in the final patterns. However, a more detailed analysis shows some slight differences between patterns obtained at high concentrations and at high temperatures. Indeed, the pigments appear uniformly distributed in a single large disc at $\phi = 16.7\%$ and $T = 30\text{ }^{\circ}\text{C}$, whereas they are found scattered in a central spot surrounded by a relatively wide ring at $\phi = 2.5\%$ and $T = 80\text{ }^{\circ}\text{C}$. This slight difference suggests that temperature and concentration do not equivalently affect the mechanisms at play.

Mechanisms at Play. To deepen the understanding of the kinetics of drop evaporation and the resulting pigment patterns, we investigate two aspects: the first deals with the evaporation mechanisms and the pigment's organization inside the dried drop; the second concerns the rheological properties of the paint suspensions and the sol–gel transition as the suspension concentration increases.

Evaporation Mechanisms. We here focus on the different evaporative flows generated within the sessile drop and their contribution to the shape of the final deposit. For this purpose, it is important to keep in mind the main features of our system:

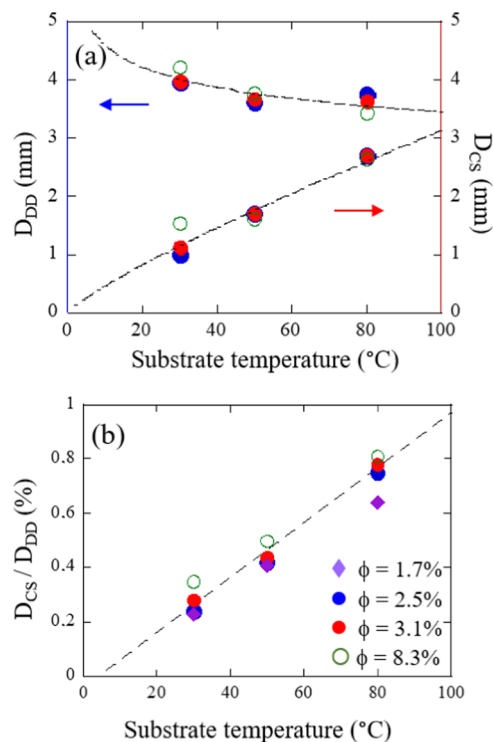


Figure 4. Analysis of the final dried drops: (a) diameters of central stain (D_{CS}) and dried drop (D_{DD}) as a function of the substrate temperature for different volume concentrations ϕ . (b) Diameter of the central stain (D_{CS}) normalized by the diameter of the dried drop as a function of the substrate temperature. Each point is an average of at least 10 measurements, and the error bar is smaller than the symbol size.

(i) the drop evaporation occurs on heated substrates, which generates a temperature gradient along the liquid–vapor interface. The corresponding gradient in surface tension induces an inward thermal Marangoni flow from the hot region toward the cool region (the drop apex). (ii) The investigated suspensions are a mixture of small pigments and liquids. A spatial accumulation of some components in the drop generates a concentration gradient. This leads to a surface tension gradient that may induce an inward solutal Marangoni flow across the drop interface. In our experiments, the existence of a solutal Marangoni flow is supported by surface tension measurements performed on a dilute suspension of paint. These measurements²⁸ show that the constituents of the paint do have a surface activity with a surface tension ranging from 43.5 ± 1 to 26.5 ± 1 mN/m for volume concentration ϕ varying between 0.5 and 10%. Thermal and solutal Marangoni flows are thus in the opposite direction to the bulk capillary flow, which ensures the particle transport to the drop edge. To understand in greater detail the impact of such inward flows on the resulting patterns, we observed in a top-view configuration

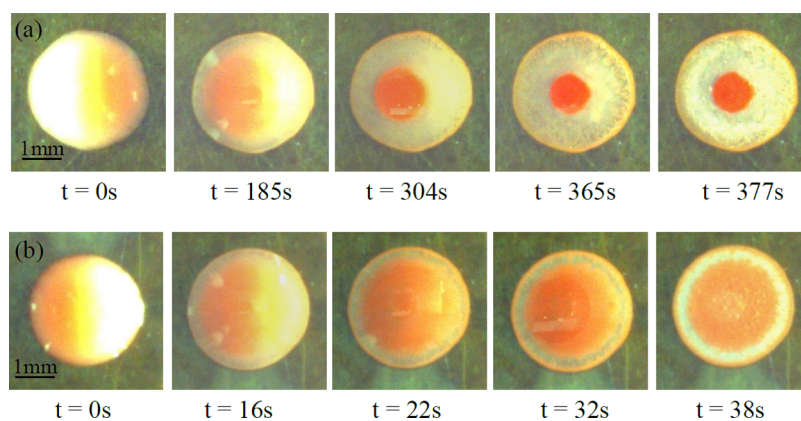


Figure 5. Time evolution of a drying drop made of paint suspension ($\phi = 1.7\%$) on glass surfaces at 30 °C (a), where a configuration like “fried eggs” is observed, and at 80 °C (b), where a more homogeneous pattern is observed.

the whole process for both low (30 °C) and high (80 °C) substrate temperatures. Figure 5a shows a typical top-view image sequence capturing the different evaporating steps of a drop of paint suspension ($\phi = 1.7\%$) on a substrate at 30 °C and its interesting particularities. Three sequential stages can be distinguished. In the first, the contact line is quickly pinned and remains in this configuration throughout the drying process. A gel-like phase develops close to the edge, while the central area remains liquid, as can be seen in the movies (see Movie 1) displayed in the Supporting Information. In the second stage (≥ 185 s at 30 °C), the pigments are mainly transported by the inward flow to the central region, which in our experiments occurs at a speed of about 2.1 $\mu\text{m/s}$. At the same time, the gelation of the suspension continuously moves inward, gradually reducing the reach of the capillary flow and consequently the transport of pigments to the edge. In the third stage corresponding to the end of the evaporation ($t \geq 365$ s), the thin liquid film retracts and the edge of the drop dries completely whose signature is the occurrence of rough patterns. Then, the drying front invades the whole drop quite rapidly (in a few tens of seconds), setting the spatial distribution of the pigments, i.e., freezing the morphology of the pattern. At 30 °C, a large amount of pigments is concentrated at the center of the drop and only a thin peripheral ring is observed, leading to a “fried-egg” configuration.

The influence of the substrate temperature on the kinetics and morphology of the evaporative drop is illustrated in Figure 5b. In this case, the whole drying process takes place in only 38 s, which is about 1 order of magnitude quicker than at $T = 30$ °C (see Movie 2 in the Supporting Information). In this faster evaporation, the propagation of both the gelation and the drying fronts is greatly accelerated, the internal flows are strongly inhibited, and a more uniform deposit morphology is achieved.

Analysis of the whole evaporation cycle shows that the patterns of the dried drops result from the competition between three phenomena: *evaporative flows* (capillary and Marangoni), *gelation of the suspension* that slows down the flows, and *final drying* of the drop that freezes the position of the pigments onto the substrates. At 30 °C, the transport of particles within the drop appears to be largely dominated by Marangoni flows (solutal and thermal are probably present). Both gelation and drying processes are here delayed in time; only a little fraction of pigments is adsorbed onto the substrate

at the drop edge, whereas the majority of pigments is concentrated at the center. In contrast, the final configuration of the deposit obtained at 80 °C is mainly controlled by the fast gelation and drying of the drop, which reduce the efficiency of the flows and lead to a more homogeneous morphology.

Finally, with these experiments, we have identified three different mechanisms (*inward/outward flows, gelation of the paint suspension, and final drying*) governing the morphology of the final pattern formation. We have also identified the temperature of the substrates as a key parameter that modulates the relative contribution of these mechanisms.

Rheology of the Paint. In order to investigate the sol–gel transition in more detail, we performed rheological measurements of paint suspensions at different volume concentrations and temperatures. Two types of measurements are done: constant shear-rate experiments that allow exploring the shear-thinning or shear-thickening behavior of the suspension and oscillatory deformations at constant frequency and strain that give information about the viscoelastic properties of the suspension.

The constant shear-rate experiments are performed at 30 °C, and the range of the explored shear rates²⁹ spans from 10 to 300 s^{-1} , and for each shear rate, the stress is measured after 10 s of flow. These parameters have been chosen to ensure both a good sensitivity of the measurement even for low viscosity ($\sim \text{mPa}\cdot\text{s}$) and a small impact of the solvent evaporation for the highly concentrated suspension. The measurements show that the paint suspensions are shear-thinning fluids, especially when the concentration is high. The flow curves are indeed well described by a power law dependence ($\sigma = K\dot{\gamma}^n$) whose power law exponent n decreases as the concentration increases.³⁰ In order to study the influence of the concentration on the viscosity, we compared the viscosity measured at the smallest measured shear rate ($\dot{\gamma} = 10 \text{ s}^{-1}$), which is reasonable with respect to the drying drop experiment. Note that it is difficult to know precisely the shear rates encountered by the suspension inside the drop; except at the first instants (less than a few seconds) and except in the proximity of the triple line (before anchoring), the shear rates are typically smaller than 1 s^{-1} . However, as explained, the evaporation of the paint suspension and the resolution of the rheometer impose a low limit for the shear rate ($\dot{\gamma} = 10 \text{ s}^{-1}$). In Figure 6, we plot the viscosity of the paint suspension as a function of volume concentration ϕ . Going from $\phi = 0$ to 100%, the viscosity gains

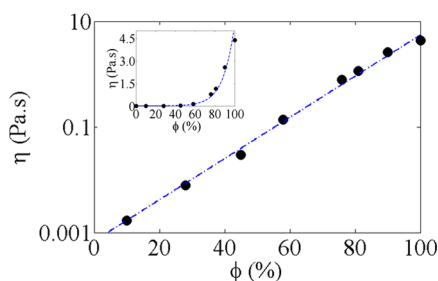


Figure 6. Viscosity of the paint suspension η (solid black circles), in the logarithmic scale, measured at $\dot{\gamma} = 10 \text{ s}^{-1}$, as a function of fraction ϕ . The inset corresponds to the plot of the viscosity as a function of the fraction in the linear scale. The dashed-dotted blue line corresponds to the fit of the data with the following equation: $\eta = \eta_0 \exp^{(a\phi - b)}$ with $\eta_0 = 1 \text{ Pa}\cdot\text{s}$, $a = 8.97$, and $b = 7.27$. The error on the viscosity is at most 10%.

more than 3 orders of magnitude. Note that the viscosity of the colloidal suspension is classically plotted as a function of the solid volume fraction ϕ_s and shows divergence at a jamming fraction ϕ_j , typically between 55 and 64% for monodisperse and spherical particles.³¹ In our study, ϕ is not the solid volume fraction and $\phi = 100\%$ just corresponds to the case of the nondiluted commercial paint.³² This implies that the concentration inside the evaporative drop can exceed the concentration of the nondiluted paint, i.e., $\phi = 100\%$, especially at the end of the evaporation. This also implies that the viscosity in the evaporative drop can exceed 4.5 Pa·s.

For each studied concentration, we also measured the viscoelastic properties characterized by the elastic modulus G' and viscous modulus G'' by imposing strain (1–10%) and frequency (1–10 Hz). For concentrations below 10%, no elastic modulus is detected. For higher concentrations, the viscoelastic behavior was measured with elastic and viscous moduli varying from 0.1 to 100 Pa, as shown in Figure 7.

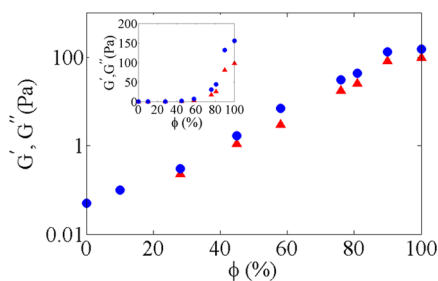


Figure 7. Elastic modulus G' (solid blue circles) and viscous modulus G'' (solid red triangles), in the logarithmic scale, measured at $f = 10 \text{ Hz}$ and $\gamma = 10\%$, as a function of the fraction ϕ of the paint suspension. The inset corresponds to the plot of the moduli as a function of the fraction in the linear scale. The error on the viscoelastic moduli is at most 10%.

Viscosity and viscoelastic moduli exhibit a strong increase with the volume concentration and gain more than 3 orders of magnitude as the concentration goes from 0 to 100%. Such divergences are well described by a linear dependence between the logarithm of the viscosity or viscoelastic moduli with the volume concentration. A divergence of the viscosity as a function of the inverse of the distance to the jamming point ($\eta \sim (\phi_j - \phi_s)^2$), classically observed with a non-Brownian suspension of rigid particles,^{33–35} is not here well verified. Such a strong increase in the viscosity with the paint concentration

gives relevant information to understand the anchoring of the drop edge and a slowing down of the flux inside the evaporative drop where paint accumulates. Moreover, the exact knowledge of the viscosity divergence with the concentration is crucial for the quantitative modeling of drop drying.

In order to study the influence of the temperature on the evaporative process, we measure the time evolution of the complex modulus $|G^*| = \sqrt{G'^2 + G''^2}$ of a paint suspension of concentration $\phi = 81\%$ at three different temperatures: $T = 30, 50,$ and $80 \text{ }^\circ\text{C}$. As shown in Figure 8, the higher the

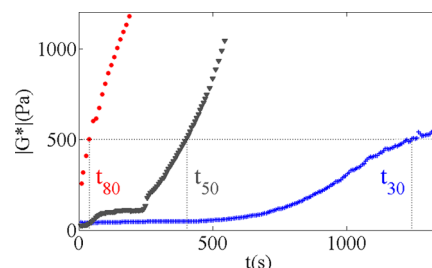


Figure 8. Time evolution of the complex modulus $|G^*|$ of a paint suspension ($\phi = 81\%$), measured at $f = 10 \text{ Hz}$ and $\gamma = 10\%$ in the cone–plate geometry, for three different substrate temperatures: $T = 30 \text{ }^\circ\text{C}$ (+), $T = 50 \text{ }^\circ\text{C}$ (black down triangles), and $T = 80 \text{ }^\circ\text{C}$ (solid red circles). The horizontal dotted line corresponds to the value of the complex modulus approximately 10 times higher than the initial one, reached after $t_{80} = 39 \text{ s}$ at $T = 80 \text{ }^\circ\text{C}$, $t_{50} = 400 \text{ s}$ at $T = 50 \text{ }^\circ\text{C}$, and $t_{30} = 1250 \text{ s}$ at $T = 30 \text{ }^\circ\text{C}$.

temperature, the steeper the increase of the complex modulus with time. To quantify this temperature dependence, we arbitrarily choose the time for which the complex modulus has been multiplied by a factor of 10 with respect to its initial value. This leads to the following times: 1250 s, 400, and 39 s, respectively, for temperatures $T = 30, 50,$ and $80 \text{ }^\circ\text{C}$. This rheological measurement indicates that the paint gelifies 3 times faster going from $T = 30$ to $50 \text{ }^\circ\text{C}$ and 30 times faster going from $T = 30$ to $80 \text{ }^\circ\text{C}$. Direct comparison between rheological measurements and drying drop experiments is not obvious since geometries are different (cone–plate for rheological measurement and spherical cap for drying drop) and surface-to-volume ratios are different (typically 160 m^{-1} for the cone–plate geometry and 750 m^{-1} for a spherical cap of radius $R_c = 2 \text{ mm}$ and $\theta = 20^\circ$). Nonetheless, the orders of magnitude of both experiments are consistent and indicate that the gelation and the drying of paint drops are at least 10 times faster at $80 \text{ }^\circ\text{C}$ than at $30 \text{ }^\circ\text{C}$ (see Figures 5 and 8).

Influence of Concentration and Temperature on the Evaporative Mechanisms. Previous results and analysis show that the patterns of the dried drops result from the interplay between three mechanisms (gelation of the paint suspension, inward/outward flows, and final drying) and their relative kinetics with concentration and temperature. In order to understand this evaporation process, we discuss in the following the influence of the concentration and temperature on each mechanism separately.

Concerning the gelation of the paint suspension, the rheological measurements have underlined a strong increase of the viscosity and the viscoelastic moduli with concentration, at least by 3 orders of magnitude as the concentration varies from 0 to 100% (from water to commercial paint). Such an

increase implies a significant slowing of the dynamics of the flows inside the drop, especially where pigments accumulate. In the case of the evaporating drop, the gelation of the suspension starts at the drop edge^{19,22,23,36,37} as capillary flow transports pigments from the center to the edge. This gelation prohibits further transport of pigments through the gel toward the contact line. This may explain why the coffee ring remains thin and stops growing quite early. Then, the gelation front progressively moves toward the center.²³ The kinetics of this propagation is controlled by the efficiency of the outward and inward flows, which strongly depend on the substrate temperature and suspension concentration. Increasing both concentration and temperature induces a stronger viscosity increase and promotes faster gelation. This can explain why increasing concentration or temperature leads to more homogeneous patterns (see Figure 2a).

Regarding inward/outward flows, their range in the drop is limited to nongelified regions. Outward capillary flows transport pigments from the center to the outside of the drop. On the contrary, the Marangoni effects at the liquid–air interface bring particles to the center, inducing inward flows in the drop. Such flows have two origins: thermal and solutal. Thermal flows result from thermal gradients inducing tension surface gradients, which are strongly enhanced as the substrate temperature is increased as shown in a previous study.¹⁵ So, in our experiments, an increase in the efficiency of the thermal Marangoni flow is expected as the temperature increases. Solutal effects are relevant and induce inward flows when the suspension exhibits surface activity and the contact line is pinned,³⁸ which is our case. Such solutal flow results from concentration gradients inducing surface tension gradients.³⁹ However, what is the influence of the suspension concentration on this solutal flow? At a low concentration of paint suspension, corresponding to a low concentration of surfactant molecules contained in the suspension, the air–liquid interface is not saturated by surfactant adsorption. This implies that gradients of surface tension between regions rich in surfactant (at the drop edge due to the constant outward capillary flow) and regions less rich (at the apex) are expected to be relevant. At a large concentration of paint suspension, corresponding to surfactant concentrations equal to or larger than the critical micellar concentration (CMC), the air–liquid interface is saturated in surfactants and the surface tension reaches a minimal value.⁴⁰ In such conditions, gradients of surface tension at the drop interface are much reduced and solutal Marangoni flows are not expected to play a significant role. Our measurements show that the surface tension of paint suspension at 10% is 26 mN/m, which is already quite low for a water-based suspension. So, we may expect that for higher concentration (>10%), the solutal Marangoni effect should not be pronounced. This analysis based on surface tension measurements suggests a decrease in the efficiency of the solutal flow with concentration.

In summary, we expect an increase in the efficiency of the thermal Marangoni flow with the temperature and a decrease in the solutal Marangoni flow with concentration. This difference in tendency may explain why increasing temperature or concentration does not lead to equivalent patterns (see Figure 2a): the central stain is still visible at high temperatures (see the pattern at 2.5% and 80 °C), which is not the case at high concentration (see the pattern at 16.7% and 30 °C).

Finally, at the end of the drop evaporation, a drying front starts at the edge of the drop and rapidly invades the whole

drop, freezing the position of the pigments and then the morphology of the dried drop. The kinetics of the front propagation is fully controlled by the substrate temperature. Indeed, the drying is 10 times faster at 80 °C than at 30 °C. This fast increase of the drying with the temperature leads to a more homogeneous pattern compared to the nonheated case.

To summarize, increasing the suspension concentration induces faster gelation and a less efficient solutal Marangoni flow, in favor of a quasi-homogeneous pattern, in agreement with the experimental findings (see patterns at 16.7% of Figure 2a). Increasing the substrate temperature induces faster gelation, faster drying, and also a more efficient thermal Marangoni flow. So, depending on the competition between these phenomena, a homogeneous pattern or pattern with a central stain can be obtained. The analyses of the patterns upon temperature (see Figure 2) indicate that increasing temperature always tends to homogenize the pigment distribution compared to the nonheated case, even if regions depleted in pigments are still visible in the final patterns (see patterns at 80 °C of Figure 2a).

CONCLUSIONS

In this paper, we have investigated the drying process of droplets made of paint suspension and the resulting patterns. In particular, we have focused our study on the influence of two parameters: the substrate temperature, ranging between 30 and 80 °C, and the suspension concentration. From our experiments, it clearly appears that the kinetics of the pattern growth results from a competition between three mechanisms: *inward/outward flows*, *gelation of the paint suspension*, and *final drying*. Their relative contribution as a function of the concentration and temperature governs the morphology of the final deposit. Our main findings are as follows: (i) in all configurations investigated, solutal and thermal Marangoni flows play a major role in the distribution of pigments. Because of this, patterns showing only a single coffee ring were never observed in our experiments. (ii) Increasing the concentration or temperature leads to faster gelation and drying of the drop. Such an effect tends to homogenize the pigment distribution in the final patterns. The only difference stands in the influence of the investigated parameters on the inward Marangoni flows: increasing concentration induces a decrease in the efficiency of the solutal Marangoni flow, whereas increasing temperature induces an increase in the efficiency of the thermal Marangoni flow. (iii) The kinetics of both *gelation* and *final drop drying* is controlled by the substrate temperature.

In addition, it must be noticed that such conclusions are supported by rheological measurements. A quantitative approach, combining optical observations and different kinds of physical measurements, has been privileged in our study. Through this, we have shown that good control of the spatial distribution of pigments in the dried drop can be obtained in a real complex fluid by a judicious choice of the two investigated parameters.

Finally, this experimental study deepens our understanding of the influence of substrate temperature and suspension concentration on the drying of drops made of a paint suspension and the mechanisms governing the distribution of the pigment in the resulting deposit. Better control of intricate mechanisms usually involved in the drying of multicomponent drops can thus be expected.

■ ASSOCIATED CONTENT

SI Supporting Information

The Supporting Information is available free of charge at <https://pubs.acs.org/doi/10.1021/acs.langmuir.3c01605>.

Drying process of a drop (given in Figure 5) on substrates at $T = 30\text{ }^{\circ}\text{C}$ (Movie 1) (AVI)

Drying process of a drop (given in Figure 5) on substrates at $T = 80\text{ }^{\circ}\text{C}$; In both movies, three sequential stages are identified: contact line pinning, suspension gelation, and final drying (Movie 2) (AVI)

■ AUTHOR INFORMATION

Corresponding Author

Stella M. M. Ramos – Université de Lyon, Université Claude Bernard Lyon 1, CNRS, Institut Lumière Matière, F-69622 Villeurbanne, France; orcid.org/0009-0003-7961-3140; Email: stella.ramos-canut@univ-lyon1.fr

Authors

Damien Soubeyrand – Université de Lyon, Université Claude Bernard Lyon 1, CNRS, Institut Lumière Matière, F-69622 Villeurbanne, France

Rémy Fulcrand – Université de Lyon, Université Claude Bernard Lyon 1, CNRS, Institut Lumière Matière, F-69622 Villeurbanne, France

Catherine Barentin – Université de Lyon, Université Claude Bernard Lyon 1, CNRS, Institut Lumière Matière, F-69622 Villeurbanne, France

Complete contact information is available at: <https://pubs.acs.org/10.1021/acs.langmuir.3c01605>

Notes

The authors declare no competing financial interest.

■ ACKNOWLEDGMENTS

It is a pleasure to thank Dr. B. Canut from the Institut National des Sciences Appliquées (INSA) at Lyon for his precious help in the profilometry measurements.

■ REFERENCES

- (1) Deegan, R. D.; Bakajin, O.; Dupont, T. F.; Huber, G.; Nagel, S. R.; Witten, T. A. Capillary flow as the cause of ring stains from dried liquid drops. *Nature* **1997**, *389*, 827–829.
- (2) Pauchard, L.; Parisse, F.; Allain, C. Influence of salt content on crack patterns formed through colloidal suspension desiccation. *Phys. Rev. E* **1999**, *59*, 3737–3740, DOI: [10.1103/PhysRevE.59.3737](https://doi.org/10.1103/PhysRevE.59.3737).
- (3) Deegan, R. D. Pattern formation in drying drops. *Phys. Rev. E* **2000**, *61*, 475–485, DOI: [10.1103/PhysRevE.61.475](https://doi.org/10.1103/PhysRevE.61.475).
- (4) Hu, H.; Larson, R. G. Marangoni effect reverses coffee-ring depositions. *J. Phys. Chem. B* **2006**, *110*, 7090–7094.
- (5) Soltman, D.; Subramanian, V. Inkjet-printed line morphologies and temperature control of the coffee ring effect. *Langmuir* **2008**, *24*, 2224–2231.
- (6) Bigioni, T. P.; Lin, X.-M.; Nguyen, T. T.; Corwin, E. I.; Witten, T. A.; Jaeger, H. M. Kinetically driven self assembly of highly ordered nanoparticle monolayers. *Nat. Mater.* **2006**, *5*, 265–270.
- (7) Sefiane, K. On the formation of regular patterns from drying droplets and their potential use for bio-medical applications. *J. Bionic Eng.* **2010**, *7*, S82–S93.
- (8) Yunker, P. J.; Still, T.; Lohr, M. A.; Yodh, A. Suppression of the coffee-ring effect by shape-dependent capillary interactions. *Nature* **2011**, *476*, 308–311.
- (9) Ryu, S.-a.; Kim, J. Y.; Kim, S. Y.; Weon, B. M. Drying-mediated patterns in colloid-polymer suspensions. *Sci. Rep.* **2017**, *7*, No. 1079, DOI: [10.1038/s41598-017-00932-z](https://doi.org/10.1038/s41598-017-00932-z).
- (10) Orejon, D.; Sefiane, K.; Shanahan, M. Stick–slip of evaporating droplets: substrate hydrophobicity and nanoparticle concentration. *Langmuir* **2011**, *27*, 12834–12843.
- (11) Fukai, J.; Ishizuka, H.; Sakai, Y.; Kaneda, M.; Morita, M.; Takahara, A. Effects of droplet size and solute concentration on drying process of polymer solution droplets deposited. *Int. J. Heat Mass Transfer* **2006**, *49*, 3561–3567.
- (12) Parsa, M.; Harmand, S.; Sefiane, K.; Biggerelle, M.; Deltombe, R. Effect of substrate temperature on pattern formation of nanoparticles from volatile drops. *Langmuir* **2015**, *31*, 3354–3367.
- (13) Patil, N. D.; Bange, P. G.; Bhardwaj, R.; Sharma, A. Effects of substrate heating and wettability on evaporation dynamics and deposition patterns for a sessile water droplet containing colloidal particles. *Langmuir* **2016**, *32*, 11958–11972.
- (14) Shi, J.; Yang, L.; Bain, C. D. Drying of ethanol/water droplets containing silica nanoparticles. *ACS Appl. Mater. Interfaces* **2019**, *11*, 14275–14285.
- (15) Li, Y.; Lv, C.; Li, Z.; Quéré, D.; Zheng, Q. From coffee rings to coffee eyes. *Soft Matter* **2015**, *11*, 4669–4673.
- (16) Parsa, M.; Harmand, S.; Sefiane, K. Mechanisms of pattern formation from dried sessile drops. *Adv. Colloid Interface Sci.* **2018**, *254*, 22–47.
- (17) Wang, Z.; Orejon, D.; Takata, Y.; Sefiane, K. Wetting and evaporation of multicomponent droplets. *Phys. Rep.* **2022**, *960*, 1–37.
- (18) Sobac, B.; Brutin, D. Structural and evaporative evolutions in desiccating sessile drops of blood. *Phys. Rev. E* **2011**, *84*, No. 011603.
- (19) Hertaeg, M. J.; Tabor, R. F.; Routh, A. F.; Garnier, G. Pattern formation in drying blood drops. *Philos. Trans. R. Soc., A* **2021**, *379*, No. 20200391.
- (20) Woolley, A. T.; Kelly, R. T. Deposition and characterization of extended single-stranded DNA molecules on surfaces. *Nano Lett.* **2001**, *1*, 345–348.
- (21) Plisson, J. S.; de Viguierie, L.; Tahroucht, L.; Menu, M.; Ducouret, G. Rheology of white paints: How Van Gogh achieved his famous impasto. *Colloids Surf., A* **2014**, *458*, 134–141, DOI: [10.1016/j.colsurfa.2014.02.055](https://doi.org/10.1016/j.colsurfa.2014.02.055).
- (22) Giorgiutti-Dauphiné, F.; Pauchard, L. Drying drops. *Eur. Phys. J. E* **2018**, *41*, No. 32, DOI: [10.1140/epje/i2018-11639-2](https://doi.org/10.1140/epje/i2018-11639-2).
- (23) Bodiguel, H.; Leng, J. Imaging the drying of a colloidal suspension. *Soft Matter* **2010**, *6*, 5451–5460.
- (24) Bacchin, P.; Brutin, D.; Davaille, A.; Di Giuseppe, E.; Chen, X. D.; Gergjanakis, L.; Giorgiutti-Dauphiné, F.; Goehring, L.; Hallez, Y.; Heyd, R.; Jeantet, R.; Le Floch-Fouéré, C.; Meireles, M.; Mittelsedt, E.; Nicloux, C.; Pauchard, L.; Saboungi, M.-L. Drying colloidal systems: Laboratory models for a wide range of applications. *Eur. Phys. J. E* **2018**, *41*, No. 94, DOI: [10.1140/epje/i2018-11712-x](https://doi.org/10.1140/epje/i2018-11712-x).
- (25) Zang, D.; Tarafdar, S.; Tarasevich, Y. Y.; Choudhury, M. D.; Dutta, T. Evaporation of a Droplet: From physics to applications. *Phys. Rep.* **2019**, *804*, 1–56.
- (26) Janas, A.; Mecklenburg, M. F.; Fuster-López, L.; Kozłowski, R.; Kékicheff, P.; Favier, D.; Anders, C. K.; Scharff, M.; Bratasz, L. Shrinkage and mechanical properties of drying oil paints. *Heritage Sci.* **2022**, *10*, No. 181, DOI: [10.1186/s40494-022-00814-2](https://doi.org/10.1186/s40494-022-00814-2).
- (27) de Polo, G.; Walton, M.; Keune, K.; Shull, K. R. After the paint has dried: a review of testing techniques for studying the mechanical properties of artists' paint. *Heritage Sci.* **2021**, *9*, No. 68, DOI: [10.1186/s40494-021-00529-w](https://doi.org/10.1186/s40494-021-00529-w).
- (28) For concentration higher than 10%, surface-tension measurements are made difficult due to the too slow relaxation of the drop shape.
- (29) Ascending and descending ramps of 10 shear rates, spaced logarithmically, are performed.
- (30) The exponent n varies from 0.93 to 0.51 as the concentration increases from 10% to 100%.
- (31) Silbert, L. E. Jamming of frictional spheres and random loose packing. *Soft Matter* **2010**, *6*, 2918–2924.

(32) The conversion between ϕ and ϕ_s can be estimated. Complete drying of nondiluted paint shows that the solid weight fraction is $57 \pm 2\%$. Knowing the paint density (1.45) and assuming that only water evaporates, the solid volume fraction ϕ_s of nondiluted paint ($\phi = 100\%$) can be evaluated to 37%.

(33) Krieger, I. M.; Dougherty, T. J. A mechanism for non-Newtonian flow in suspensions of rigid spheres. *Trans. Soc. Rheol.* **1959**, *3*, 137–152.

(34) Boyer, F.; Guazzelli, É.; Pouliquen, O. Unifying suspension and granular rheology. *Phys. Rev. Lett.* **2011**, *107*, No. 188301.

(35) Blanc, F.; d'Ambrosio, E.; Lobry, L.; Peters, F.; Lemaire, E. Universal scaling law in frictional non-Brownian suspensions. *Phys. Rev. Fluids* **2018**, *3*, No. 114303.

(36) Okuzono, T.; Kobayashi, M.; Doi, M. Final shape of a drying thin film. *Phys. Rev. E* **2009**, *80*, No. 021603.

(37) Sobac, B.; Brutin, D. Desiccation of a sessile drop of blood: Cracks, folds formation and delamination. *Colloids Surf, A* **2014**, *448*, 34–44.

(38) Gelderblom, H.; Diddens, C.; Marin, A. Evaporation-driven liquid flow in sessile droplets. *Soft Matter* **2022**, *18*, 8535–8553.

(39) Kim, H.; Boulogne, F.; Um, E.; Jacobi, I.; Button, E.; Stone, H. A. Controlled Uniform Coating from the Interplay of Marangoni Flows and Surface-Adsorbed Macromolecules. *Phys. Rev. Lett.* **2016**, *116*, No. 124501, DOI: [10.1103/PhysRevLett.116.124501](https://doi.org/10.1103/PhysRevLett.116.124501).

(40) Rosen, M. J.; Kunjappu, J. T. *Surfactants and Interfacial Phenomena*; John Wiley & Sons, Inc., 2012.